Volume 5, Number 3
1004-423X/96/05030185-10

ACTA PHYSICA SINICA
(Overseas Edition)

March, 1996

WHISPERING-GALLERY MODE STRUCTURE IN SEMICONDUCTOR MICRODISK LASERS AND CONTROL OF THE SPONTANEOUS EMISSION FACTOR*

GUO CHANG-ZHI(郭长志)
Department of Physics, Peking University, Beijing 100871, China

CHEN SHUI-LIAN(陈水莲)
Department of Applied Mathematics, Tsinghua University, Beijing 100084, *China*

(Received 11 March 1995)

The mode density and cross-sectional area of whispering-gallery modes of various possible polarizations existing in a microdisk cavity structure have been investigated and compared in some detail. Their variations with the disk thickness and radius have been calculated and the behavior of the spontaneous emission factor controlled by the microdisk structure have been shown. It is found that for a given microdisk thickness, the spontaneous emission factor increases with decreasing microdisk radius, but decreases after passing a maximum value. This non-monotonic behavior has never been noted before by others. The variation of spontaneous emission factor with respect to microdisk thickness also exhibits similar behavior. For a microdisk laser emitting at 1.5 μm wavelength, the enhanced spontaneous emission factor can barely exceed 0.2. A device configuration for improving the coupling between the whispering-gallery mode and the active region, and for leading the laser beam out of this high-Q microcavity is proposed, and its feasibility in realizing a thresholdless laser is discussed.

PACC: 4255P; 4260D; 6865

I. INTRODUCTION

Efforts to lower the lasing threshold have always been a driving force in the development of semiconductor lasers. By using the heterojunction structure to improve spatial confinement of photons and injected carriers, the lasing threshold current density was lowered to the level of 1000 A/cm^2, and room temperature lasing was realized. With lattice-matched and strained layer quantum wells, which increase the differential optical gain and decrease the transparency current density and cavity loss, the threshold current density was lowered to the level of 50 A/cm^2. The threshold current can even be lowered to somewhat less than 1 mA if the end faces of the laser are coated with high reflectivity films.[1] It has been proposed recently to further lower the lasing threshold current and power consumption to realize large-scale optical integration and the ideal of a thresholdless semiconductor laser through control of the spontaneous emission factor by microcavity.

The proposed possible microcavity structures are mainly of three types[2], two of which have already been implemented in experimental samples, namely, the vertical-cavity surface emitting laser (VCSEL) with distributed Bragg reflector (DBR) end mirrors, and the

*Project supported by the National Natural Science Foundation of China.

microdisk laser with whispering-gallery modes. The third type, still under theoretical investigation, is the periodic dielectric micro-structure with defect modes in the photonic bandgap. Which one of the above is more feasible in practice will be determined by its degree of technological difficulty and its effectiveness in spontaneous emission factor control, etc.

The spontaneous emission factor is the fraction of photons, spontaneously emitted due to photon or electron injected non-equilibrium carrier recombination (stimulated by vacuum field fluctuations) which are coupled into a single guided lasing mode of the semiconductor laser cavity. This fraction is very small, about 10^{-5}-10^{-4} in an ordinary semiconductor laser, but it softens the optical output power-curren characteristics, widens both the laser spectral bandwidth and individual linewidths, reduces both the relaxation oscillation and modulation resonance peak, etc. However, it has no significant influence on the lasing threshold in this realm[3,4], its effect on lowering the lasing threshold becoming significant only when it increases to above 10^{-2}. The lasing threshold will even become zero when it approaches 1, that is, when all the spontaneous emission photons are coupled into a single lasing mode, which then becomes perfectly coherent and the lasing will be in a thresholdless ideal state. Therefore, to increase the spontaneous emission factor near to or up to 1 may be said to be the necessary condition for realizing an extraordinary low threshold or even thresholdless lasing. The relationships between the structure, including the polarization, mode density and mode cross-sectional area of the whispering-gallery mode in the microdisk cavity structure, and its influence in controlling the spontaneous emission factor, the mode selectivity of the microdisk structure and its improvement, and the attainable upper limit of the spontaneous emission factor will be investigated theoretically in this work and compared with the theoretical results obtained by other recent methods.[5]

II. THEORY

The available theory of the spontaneous emission factor, γ, is either formulated by classical field theory based on Maxwell's equations[7,8] or by quantum field theory based on full quantum mechanics.[9,10] Both theories are related to the structure of the lasing guided modes coupled by the spontaneous emission in any waveguiding cavity, including the polarizations, mode distributions, cross-sectional areas, and densities. In principle, these structural quantities can be obtained quite accurately by solving the classical Maxwell equations with the appropriate boundary conditions. For a circular cylindrical dielectric disk of thickness d, radius a, and refractive index $\overline{n}_2$, immersed in a surrounding medium of refractive index $\overline{n}_1$, according to the full quantum mechanical theory and after eliminating quantities related to the vacuum field fluctuations, etc., by using a certain normalization procedure[9,10], the main relationship between the spontaneous emission factor and the mode structure can

be expressed as

$$\gamma = C_n \frac{\rho_{\frac{a}{\lambda_0}}}{(\frac{w_z}{\lambda_0})(\frac{w_r}{\lambda_0})} , \quad C_n \approx \frac{3}{8\pi^2 \overline{n}_2^3} , \tag{1}$$

where λ_0 is the vacuum wavelength of the lasing guided mode, $\rho_{\frac{a}{\lambda_0}}$ is the mode density in the phase space of vacuum wavenumber $\frac{a}{\lambda_0}$, which is the inverse of the vacuum wavelength normalized by the disk radius a, w_z and w_r are the mode widths along the axial and radial directions of the disk, respectively. For a circular cylindrical coordinate system (r, φ, z) with the z axis coinciding with the disk axis, the electric and magnetic field components of the guided mode in the circular disk at instant t can be expressed as

$$F = R(r)\Phi(\phi)Z(z)T(t) . \tag{2}$$

For a harmonic wave with circular frequency, ω, the time factor can be taken as $T(t) = e^{i\omega t}$, and for a running mode propagating along the central z axis, the factor containing z can be taken as $Z(z) = e^{\pm i\beta_z z}$. The stationary wave field with harmonic function $\cos(\beta_z z)$ or $\sin(\beta_z z)$ along the z-direction in the disk is just the superposition of these two running waves propagating in opposite directions. In the case of a very thin disk ($d \ll a$), this common factor of the circular disk mode can be first solved by using an equivalent three-layer slab waveguide with inner and outer refractive indices $\overline{n}_2$ and $\overline{n}_1$, respectively.[6] Its fundamental mode exists singly within a critical thickness $d_c = \frac{\lambda_0}{2\sqrt{\overline{n}_2^2 - \overline{n}_1^2}}$, its pth order mode refractive index is $\overline{n}_z = \frac{\beta_z}{k_0}$, with vacuum wavenumber $k_0 = \frac{2\pi}{\lambda_0} = \frac{\omega}{c_0}$, where c_0 is the vacuum light velocity, and β_z is the propagation constant of the mode along the z-direction. The factor containing φ satisfies

$$\frac{1}{\Phi(\phi)} \frac{d^2\Phi(\phi)}{d\phi^2} = -m^2 , \quad \Phi(\phi) = e^{\pm im\phi} , \tag{3}$$

with period 2π. Here m is a positive integer, $+m$ and $-m$ are related to the mth order rotating running waves, also called whispering-gallery modes rotating in the left-and right-senses, with stationary wave solutions $\cos(m\varphi)$ and $\sin(m\varphi)$, respectively. The factor $R(r)$ satisfies a Bessel equation,

$$\frac{d^2R(r)}{dr^2} = \frac{1}{r}\frac{dR(r)}{dr} + \left(k_j^2 - \frac{m^2}{r^2}\right) R(r) = 0 , \quad k_j^2 = k_0^2(\overline{n}_j^2 - \overline{n}_z^2) . \tag{4}$$

$R(r)$ in the electric and magnetic field components of the whispering-gallery modes with different polarizations can be written as

$$E_{z2}^{mn}(r) = J_m\left(u\frac{r}{a}\right) F_{z2}^{E_{mn}} , \quad E_{z1}^{mn}(r) = \frac{J_m(u)}{K_m(w)} K_m\left(w\frac{r}{a}\right) F_{z1}^{E_{mn}} , \tag{5a}$$

$$H_{z2}^{mn}(r) = iJ_m\left(u\frac{r}{a}\right) F_{z2}^{H_{mn}} , \quad H_{z1}^{mn}(r) = i\frac{J_m(u)}{K_m(w)} K_m\left(w\frac{r}{a}\right) F_{z1}^{H_{mn}} , \tag{5b}$$

$$E_{r2}^{mn}(r) = -\mathrm{i}J_m\left(u\frac{r}{a}\right)F_{r2}^{E_{mn}}\ , \quad E_{r1}^{mn}(r) = \mathrm{i}\frac{J_m(u)}{K_m(w)}K_m\left(w\frac{r}{a}\right)F_{r1}^{E_{mn}}\ , \tag{5c}$$

$$E_{\phi 2}^{mn}(r) = J_m\left(u\frac{r}{a}\right)F_{\phi 2}^{E_{mn}}\ , \quad E_{\phi 1}^{mn}(r) = -\frac{J_m(u)}{K_m(w)}K_m\left(w\frac{r}{a}\right)F_{\phi 1}^{E_{mn}}\ , \tag{5d}$$

$$H_{r2}^{mn}(r) = J_m\left(u\frac{r}{a}\right)F_{r2}^{H_{mn}}\ , \quad H_{r1}^{mn}(r) = -\frac{J_m(u)}{K_m(w)}K_m\left(w\frac{r}{a}\right)F_{r1}^{H_{mn}}\ , \tag{5e}$$

$$H_{\phi 2}^{mn}(r) = -\mathrm{i}J_m\left(u\frac{r}{a}\right)F_{\phi 2}^{H_{mn}}\ , \quad H_{\phi 1}^{mn}(r) = \mathrm{i}\frac{J_m(u)}{K_m(w)}K_m\left(w\frac{r}{a}\right)F_{\phi 1}^{H_{mn}}\ , \tag{5f}$$

where the subscripts 2 and 1 refer to the quantities inside ($\overline{n}_j = \overline{n}_2$) and outside ($\overline{n}_j = \overline{n}_1$) the disk, respectively; $\mathrm{i} = \sqrt{-1}$, $n = 0, 1, 2, \cdots$ denote the nth order radial waves corresponding to a given mth order whispering-gallery mode. J_m and K_m are the mth order Bessel function of the first kind and the modified Bessel function of the second kind, respectively. The corresponding field distribution factors are

$$F_{zj}^{E_{mn}} = A_E\ , \quad F_{zj}^{H_{mn}} = A_H\ , \tag{6a}$$

$$F_{rj}^{E_{mn}} = A_1 C_{mnj}(\frac{r}{a}) + B_1 D_{mnj}(\frac{r}{a})\ , \quad F_{rj}^{H_{mn}} = A_3 C_{mnj}(\frac{r}{a}) + B_3\overline{n}_j^2 D_{mnj}(\frac{r}{a})\ , \tag{6b}$$

$$F_{\phi j}^{E_{mn}} = A_2 C_{mnj}(\frac{r}{a}) + B_2 D_{mnj}(\frac{r}{a})\ , \quad F_{\phi j}^{H_{mn}} = A_4\overline{n}_j^2 C_{mnj}(\frac{r}{a}) + B_4 D_{mnj}(\frac{r}{a})\ , \tag{6c}$$

in which, $j = 2, 1$, and

$$A_E = \frac{1}{2\pi(\frac{a}{\lambda_0})\overline{n}_z}\ , \quad A_H = (\frac{m\overline{n}_z}{c_0\mu_0})A_E\ , \quad U_w = \frac{\frac{1}{u^2}+\frac{1}{w^2}}{\frac{J'_m(u)}{uJ_m(u)}+\frac{K'_m(w)}{wK_m(w)}}\ , \tag{7a}$$

$$A_1 = 1\ , \quad A_2 = -mU_w\ , \quad A_3 = \frac{m\overline{n}_z}{c_0\mu_0}U_w\ , \quad A_4 = \frac{c_0\varepsilon_0}{\overline{n}_z}\ , \tag{7b}$$

$$B_1 = mA_2\ , \quad B_2 = mA_1\ , \quad B_3 = -mA_4\ , \quad B_4 = -mA_3\ , \tag{7c}$$

$$C_{mn2}(\frac{r}{a}) = \frac{J'_m(u\frac{r}{a})}{uJ_m(u\frac{r}{a})}\ , \quad C_{mn1}(\frac{r}{a}) = \frac{K'_m(w\frac{r}{a})}{wK_m(w\frac{r}{a})}\ , \tag{8a}$$

$$D_{mn2}(\frac{r}{a}) = \frac{1}{u^2\frac{r}{a}}\ , \quad D_{mn1}(\frac{r}{a}) = \frac{1}{w^2\frac{r}{a}}\ , \tag{8b}$$

$$u = 2\pi\frac{a}{\lambda_0}\sqrt{\overline{n}_2^2 - \overline{n}_z^2}\ , \quad w = W_u u\ , \quad W_u = \sqrt{\frac{\overline{n}_z^2 - \overline{n}_1^2}{\overline{n}_2^2 - \overline{n}_z^2}}\ . \tag{9}$$

The eigenvalues u are determined by the following eigenequations for different polarizations,

$$Z_m = -\frac{\overline{n}_2^2 + \overline{n}_1^2}{2\overline{n}_2^2}X_m \mp \sqrt{\left(\frac{\overline{n}_2^2 - \overline{n}_1^2}{2\overline{n}_2^2}\right)^2 X_m^2 + m^2\left(\frac{1}{u^2}+\frac{1}{w^2}\right)\cdot\left(\frac{1}{u^2}+\frac{\overline{n}_1^2}{\overline{n}_2^2}\frac{1}{w^2}\right)}\ , \tag{10a}$$

$$Z_m = \frac{J'_m(u)}{uJ_m(u)}\ , \quad X_m = \frac{K'_m(w)}{wK_m(w)}\ , \tag{10b}$$

where J'_m and K'_m are the derivatives of J_m and K_m with respect to the arguments shown in their parentheses, respectively. The solutions from Eq. (10) with a negative sign in front of the square root are HE_{mn} modes of hybrid polarization, and that with a positive sign are EH_{mn} modes of hybrid polarization. They become transverse electric polarized modes, TE_{0n}, and transverse magnetic polarized modes. TM_{0n}, respectively, only when $m = 0$. All these modes are solved with respect to a given pth order transverse electric polarized TE_z mode or transverse magnetic polarized TM_z mode in the z-direction.[6] They constitute, as a whole, a system of three dimensional mnpth order whispering-gallery modes with certain stationary wave distributions in the z- and r-directions while rotating along the φ-direction. The mode density in normalized wavenumber $\frac{a}{\lambda_0}$ space of a given npth order mode is

$$\rho_{\frac{a}{\lambda_0}} = \frac{\mathrm{d}m}{\mathrm{d}(\frac{a}{\lambda_0})} . \tag{11}$$

For comparison, in Eq. (3), letting

$$m\phi = a\phi k_v = a\phi k_0 \overline{n}_v , \quad \text{i.e.} , \quad k_v = \frac{m}{a} = k_0 \overline{n}_v , \tag{12}$$

the mode density in k_0 space[6] can also be found from Eq. (11) simply by putting

$$\rho_{k_0} = \frac{\mathrm{d}k_v}{\mathrm{d}k_0} = \frac{1}{2\pi}\rho_{\frac{a}{\lambda_0}} . \tag{13}$$

In the case of a microdisk with $d \leq d_c$, $p = 0$ always holds, so it is understood in the following that there is always only a single fundamental mode in the z-direction. The eigenvalues u_{mn} of the mnth order modes can be solved for a given mth order mode. The ratio

$$\alpha_{mn} = \frac{m}{u_{mn}} = \frac{r_{\min}}{a} \tag{14}$$

corresponds to the radius of the circle contacted externally by the projection of the family of skew rays in the normal cross-sectional plane of the circular cylinder. In the ray picture there is no optical rays inside this circle for $r < r_{\min}$, but in the wave picture, there still exists the damping distribution of the evanescent wave of the mode similar to that outside the disk due to the Goos-Hächen shift. Therefore, the cross-sectional widths, w_r and w_z, of the whispering-gallery mode should be measured respectively by the width between the locations of the field distribution in the r-direction damped to their respective e^{-1} values from $r = a$ outward and $r = r_{\min}$ inward, and that between the locations of the field distribution in z-direction damped to their respective e^{-1} values from $z = \pm\frac{d}{2}$ outward. The former can only be determined by numerical calculation, while the latter can be expressed analytically by[11]

$$\frac{w_z}{\lambda_0} = \frac{d}{\lambda_0} + \frac{1}{q_z \pi \sqrt{\overline{n}_2^2 - \overline{n}_i^2 - \overline{n}_z^2}} , \tag{15}$$

where $q_z = 1$ for the TE_z mode, and $q_z = (\frac{\overline{n}_z}{\overline{n}_2})^2 + (\frac{\overline{n}_z}{\overline{n}_2})^2 - 1$ for the TM_z mode.

The condition for the existence of the confined or guided modes in a microdisk waveguide is

$$\overline{n}_1 < \overline{n}_z < \overline{n}_2 \ , \tag{16}$$

which requires

$$\frac{d}{\lambda_0} < \frac{1}{2\sqrt{\overline{n}_2^2 - \overline{n}_1^2}} = \frac{d_c}{\lambda_0} \ , \quad \frac{a}{\lambda_0} > \frac{(u_{mn})_c}{2\pi\sqrt{\overline{n}_2^2 - \overline{n}_1^2}} = \frac{a_c}{\lambda_0} \ , \tag{17}$$

where $(u_{mn})_c$ is the cutoff value of u_{mn} at $\overline{n}_z = \overline{n}_1$.[11]

III. RESULTS

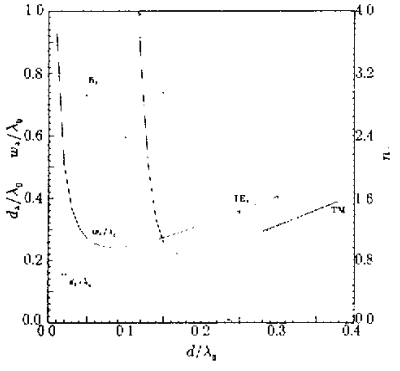

Fig. 1. Variations of the axial mode refractive index $\overline{n}_z$ (dot-dashed curves) and normalized axial mode widths $\frac{w_z}{\lambda_0}$ (solid curves) and $\frac{d_z}{\lambda_0}$ (dashed curve) versus normalized microdisk thicknesses $\frac{d}{\lambda_0}$ ($p = 0$).

Consider a typical configuration to enhance the optical confinement for a long wavelength semiconductor laser lasing at 1.5 μm, and assume the cavity simply consists of a quartenary solid solution crystal, InGaAsP, with $\overline{n}_2 = 3.4$, immersed in air of $\overline{n}_1 \approx 1$, which gives $\frac{d_c}{\lambda_0} = 0.4$ and $\frac{a_c}{\lambda_0} = 0.15$. The calculated variations of the mode indices $\overline{n}_z$ of the fundamental ($p = 0$) TE$_z$ and TM$_z$ modes with the microdisk thickness normalized by the vacuum wavelength, $\frac{d}{\lambda_0}$, are shown in Fig. 1, which also shows the corresponding normalized widths in the z-direction, $\frac{w_z}{\lambda_0}$ (solid curves), and those obtained by cosine fitting, $\frac{d_z}{\lambda_0} = \frac{1}{2\overline{n}_z}$ (dashed curves). The eigenvalues u_{mn} solved for a given mth order whispering-gallery mode of different polarizations and different nth orders for different normalized microdisk thicknesses

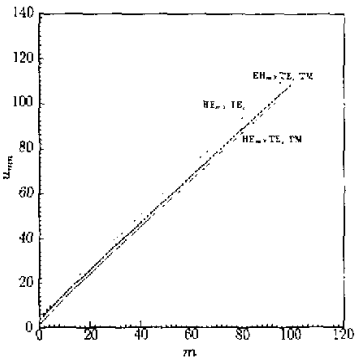

Fig. 2. Variation of the eigenvalue u_{mn} of the $mnpth$ order whispering-gallery modes ($p = 0$) versus mode order m, for different polarization and different normalized thicknesses. $\frac{d}{\lambda_0} = 0.01, 0.05, 0.1, 0.14$.

are shown in Fig. 2, which shows almost no difference for different disk thicknesses. The relation between mode order m for different polarizations and different microdisk thicknesses and the normalized microdisk radius, $\frac{a}{\lambda_0}$, is shown in Fig. 3(a). The vacuum wavelength λ_0 of the mth order whispering-gallery mode when $a = 2\,\mu m$ and $n = 0$ is shown in Fig. 3(b). It can be seen that the mode with lasing wavelength $\lambda_0 = 1.5\,\mu m$ can only be of high order. The thicker the disk, the higher the mode order m becomes, with the order m of the HE_{m0}-TE_z polarization being the highest, i.e., the stationary wave pattern will be in the form of an optical ring consisting of $2(m+1)$ spots along and near the circular edge. The shorter the wavelength, the higher the mode order m. Moreover, in a three-dim-

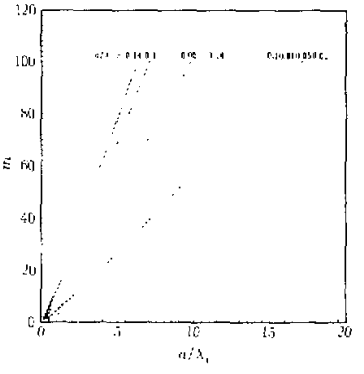

(a) Variation of whispering-gallery mode order m of different polarizations, HE_{m0}-TE_z (solid curves), HE_{m0}-TM_z (dashed curves), EH_{m0}-TE_z (dot-dashed curves), EH_{m0}-TM_z (dotted curves), versus normalized microdisk radius $\frac{a}{\lambda_0}(p = 0)$.

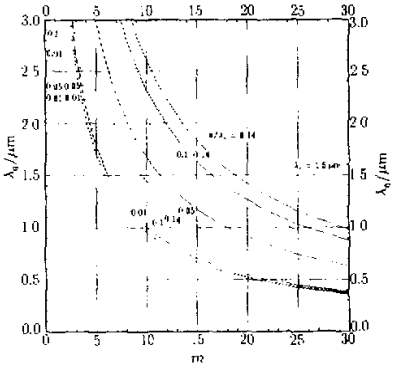

(b) Variation of the lasing wavelength λ_0 in a microdisk of radius $a = 2\,\mu m$ versus mode order m, for different normalized thicknesses $\frac{d}{\lambda_0}$ and different polarizations as Fig. 3(a) ($p = 0$).

Fig. 3. Variation of whispering mode order and the lasing wavelength.

ensional waveguide microdisk with a given structure $(\frac{d}{\lambda_0}, \frac{a}{\lambda_0})$, there is only one wavelength for each mode of $pmnth$ order. The relation between u_{mn} and $\frac{a}{\lambda_0}$ is similar to that shown in Fig. 3(a). The variation of the ratio $\alpha_{mn} = \frac{m}{u_{mn}} = \frac{r_{min}}{a}$ with $\frac{a}{\lambda_0}$ is shown in Fig. 4(a). It is seen from Fig. 3(a) that the higher the mode order m, the nearer the optical field approaches the circular edge; and the thinner the disk, the more prominent the phenomenon. For

example, the radial electric field distribution of the mode is shown in Fig. 4(b) with $m = 10$

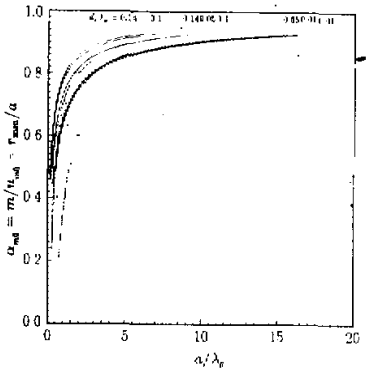

(a) Variation of normalized radius $\frac{r_{min}}{a}$ of the circle contacted externally by the projection of the family of skew rays on the cross-section versus normalized microdisk radius $\frac{a}{\lambda_0}$, for different thicknesses $\frac{d}{\lambda_0}$ and different polarizations as Fig. 3(a) ($p = 0$).

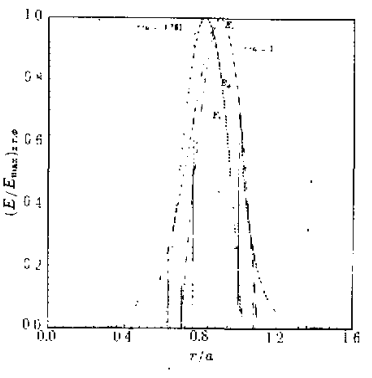

(b) The spatial distribution of the field components of HE_{mn}-whispering-gallery mode of $m = 10$, $n = 0$, $p = 0$ with $\frac{d}{\lambda_0} = 0.14$, $\frac{a}{\lambda_0} = 0.76788$, $\overline{n}_g = 2.03386$, and their corresponding normalized radial mode widths $\frac{w_r}{a}$ and $\frac{w_c}{a}$ obtained by different standards, the latter is obtained by cosine fitting. The results are $\frac{w_r}{a} = 0.446, 0.490, 0.499$, and $\frac{w_c}{a} = 0.406, 0.395, 0.410$ for E_z, E_r, E_ϕ, respectively.

Fig. 4

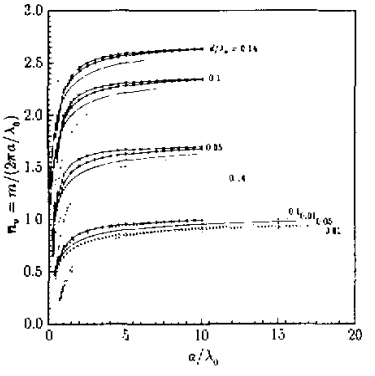

(a) Variation of $\overline{n}_v$ of whispering-gallery modes versus normalized microdisk radius $\frac{a}{\lambda_0}$ for different normalized microdisk thicknesses $\frac{d}{\lambda_0}$, and different polarizations as Fig. 3(a) ($p = 0$). Results by conformal mapping (curves with circles), and that by using formula, $\alpha = 0.984 - 0.163\frac{\lambda}{a}$, (curves with $\times$) are shown for comparison.

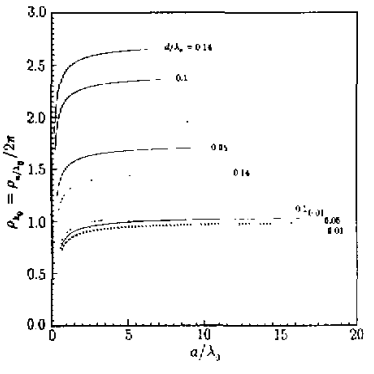

(b) Variation of mode densities, ρ_{k_0} and $\rho_{\frac{a}{\lambda_0}}$, of whispering-gallery modes versus normalized microdisk radius $\frac{a}{\lambda_0}$, for different normalized microdisk thicknesses $\frac{d}{\lambda_0}$ and different polarizations as Fig. 3(a) ($p = 0$).

Fig. 5

and $\frac{d}{\lambda_0} = 0.14$, which also compares the mode width w_c obtained by cosine fitting, with the mode width w_r obtained by including the Goos-Hächen shift. The variations of $\overline{n}_v$ and mode density with microdisk radius for different microdisk thicknesses and polarizations are shown in Figs. 5(a) and 5(b) respectively. The corresponding spontaneous emission factor obtained are shown in Fig. 6, which also shows the results by Chin *et al.* using a simplified model and conformal mapping.[6] It can be seen that their simplified model overestimated the possible values of the spontaneous emission factor, which increases monotonically with decreasing microdisk radius (Fig. 6). This is of course not reasonable, and is probably due to neglecting of the Goos-Hächen shift (Fig. 1), and also due to their approximation which overestimates the mode density (Fig. 6). In fact, for $m \neq 0$, there are only hybrid polarized modes in the microdisk, and no TE_{0n} or TM_{0n} polarized modes can exist at all. The Goos-Hächen shift widens the mode width, especially when the geometrical width of the cavity is narrow, so that the spontaneous emission factor will increase with decreasing microdisk radius and thickness up to a maximum, and then begin to decrease due to significant widening of the mode width by the Goos-Hächen shift in a cavity of small geometrical width.

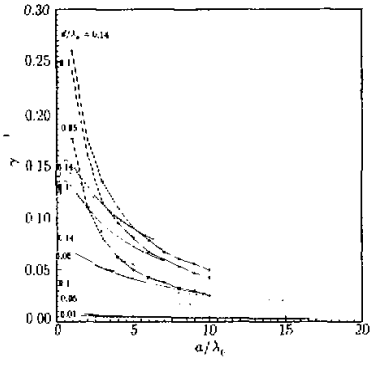

Fig. 6. Variation of the spontaneous emission factor γ of whispering-gallery modes versus normalized microdisk radius $\frac{a}{\lambda_0}$, for different normalized microdisk thicknesses $\frac{d}{\lambda_0}$ and different polarizations as Fig. 3(a) ($p = 0$). Results by Chin *et al.*[6] (curves with circles) are shown for comparison.

As the optical field of the whispering-gallery mode is concentrated in a region near the disk edge where $r_{\min} < r < a$, the uniformly injected carriers in the central $r < r_{\min}$ area will stay outside the optical field and can give no contribution to stimulated recombination. To improve the coupling between the mode field and injected non-equilibrium carriers, it is proposed that the upper electrode should be in the form of a circle with a radius somewhat smaller than $r_{\min}$, and the lower electrode should be in the form of an annulus of inner radius $r_{\min}$ and outer radius a, so as to guide the distribution of injected non-equilibrium carriers to coincide with that of the whispering-gallery mode field. Since the refractive index difference given in this case is very large, the radial optical field is damped so rapidly outside the lateral edge boundary of the microdisk that it is not easy to couple out the laser output. This is indeed a difficult problem for this kind of semiconductor laser of high-Q microdisk structure. However, in the case of a very thin disk, there may still be a strong enough whispering-gallery mode field in the axial distribution (Fig. 1) outside the upper and lower surfaces of the disk, so that it may be possible to lead out the laser beam by an optical fiber. The details of this design and its corresponding characteristics will be discussed in another article.

IV. CONCLUSION

The mode density and mode cross-sectional area have been calculated from the solutions of strictly circular cylindrical waveguiding modes under thin disk conditions. Their influence on the control of the spontaneous emission factor of whispering-gallery mode in a microdisk cavity is discussed. It is found that, by considering the Goos-Hänchen shift, the spontaneous emission factor of a mode of any polarization not only has a maximum with respect to varying microdisk thickness, but also has a maximum with respect to varying microdisk radius. This will set an upper limit to the spontaneous emission factor. Even for the HE_{m0}-TE_z polarized mode which has a higher spontaneous emission factor, its maximum value at $\frac{d}{\lambda_0} = 0.14$ and $\frac{a}{\lambda_0} = 0.45$ is only $\gamma = 0.165$, less than $\gamma = 0.2$. A device configuration is proposed which can minimize the lasing threshold and couple out the laser beam in a microdisk cavity. However, even after all kinds of possible improvements have been used and the lasing threshold has been lowered considerably, it still seems extremely difficult for a microdisk semiconductor laser to become a thresholdless laser.

REFERENCES

[1] C. Z. Guo, Semiconductor Quantum Well Lasers, Workshop on Semiconductor Superlattice/Quantum Well Physics and Opto-Electronic Devices (Guangzhou, Jan. 1991).
[2] Y. Yamamoto, R. E. Slusher, *Physics Today*, (June 1993), 66.
[3] C. Z. Guo, J. C. Niu, *Chin. J. Semicond.*, **4**(1983), 247.
[4] Y. G. Zhao, C. Z. Guo, *Chin. J. Semicond.*, **10**(1989), 254.
[5] S. L. McCall, A. F. J. Levi, R. E. Slusher, S. J. Pearton, R. A. Logan, *Appl. Phys. Lett.*, **60**(1992), 289.
[6] M. K. Chin, D. Y. Chu, S. T. Ho, *J. Appl. Phys.*, **75**(1994), 3302.
[7] Y. Suematsu, K. Furuya, *Trans. IECE Japan*, **E60**(1977), 467.
[8] K. Petermann, *IEEE J. Quantum Electron.*, **QE-15**(1979), 566.
[9] Y. Yamamoto, S. Machida, G. Björk, *Opt. Quantum Electron.*, **24**(1992), S215.; H. Yokoyama *et al.*, *ibid.*, S245.
[10] A. Y. Chu, S. T. Ho, *Opt. Soc. Am.*, **B10**(1993), 381.
[11] C. Z. Guo, Semiconductor Laser Mode Theory (in Chinese) (Beijing: People's Posts and Communication Press, Dec. 1989).